ADD-ON LOOP SHAPING VIA YOULA PARAMETERIZATION FOR PRECISION MOTION CONTROL

Xu Chen[1], **and Masayoshi Tomizuka**[1]
[1]**Department of Mechanical Engineering**
University of California, Berkeley
Berkeley, California, USA

INTRODUCTION

Advances in manufacturing are urging the innovation of new hardware and software in precision motion control systems. In the year of 2011, the manufacturing sector generated 12.2% of total U.S. GDP [1]. This percentage is additionally projected to increase greatly in future [1]. As a result, the continuously updated requirement of higher speed and higher accuracy has placed new challenges for servo design, where standard feedback control techniques alone (such as PID and H_∞ control) are commonly not sufficient to achieve the performance requirements [2].

In this paper, we discuss add-on loop-shaping ideas via Youla parameterization, aka all stabilizing controller parameterization, for improved servo performance. Loop shaping here refers to the frequency-domain servo design concept about shaping the closed-loop dynamic behavior. We present the design of flexible Youla parameterization to address common control challenges in precision motion control. Specifically, we show that the important problems of repetitive control, active vibration rejection, and bandwidth adjustment, can be uniformly formulated in the same loop-shaping scheme via Youla parameterization. One particular advantage of such a controller formulation is that stability and servo performance can be approximately separated, yielding an intuitive and performance-orientated design.

The discussed algorithms are best suited for precision control systems where the system dynamics are linear time invariant, and an accurate system model is available (from, e.g., system identification and finite element analysis). High sampling rate, accurate sensors, and precision actuators are common features of these systems. One example is the wafer scanner for lithography in the semiconductor industry. We will use an experimental setup of such a system for algorithm verification later in the paper. The proposed selection of Youla structure has also been successfully applied to hard disk drives [4], active suspensions [3], and electrical power steering in automotive vehicles [6]. The unified analysis for different loop-shaping schemes and the detailed implementation steps on the wafer scanner however have not been discussed before.

THE DESIRED LOOP SHAPE

To motivate Youla parameterization, consider a general feedback closed loop as shown in Fig. 1. To let the output y follow the reference r while rejecting the disturbances d and d_o, the controller C is designed such that $G_{r\to y}$, the transfer function from y to r, approximates unity; and the transfer functions from the disturbances to y are maintained small. The two problems about reference tracking and disturbance regulation are connected by the sensitivity function $S \triangleq 1/(1+PC)$–the transfer function from d_o to y. Standard PID and H_∞ design can readily achieve a magnitude response of S as shown in Fig. 2: it has small gains below the bandwidth ω_c, where disturbances are attenuated and $G_{r\to y} = PC/(1+PC) = 1 - S \approx 1$.

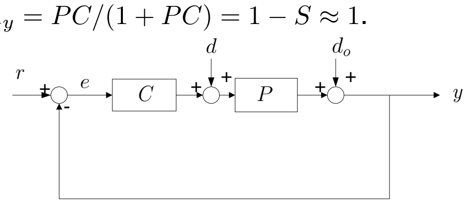

FIGURE 1. Standard feedback design structure

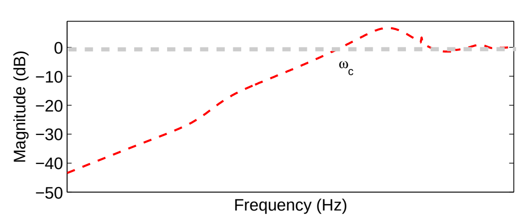

FIGURE 2. Magnitude response of a standard sensitivity function

Due to imperfections in mechanical components and the operation environments, one single controller is commonly not sufficient for all tasks in an actual system. For micro/nano scale precision servo, feedback design has to be customized as much as possible by considering characteristics of the disturbance and the control task. Fig. 3 shows an example loop shape that is customized for enhanced servo performance at a local frequency region. The solid line is from a standard design. The dashed/dotted lines are the modified versions. Following the preceding discussions, in the notch-shape region around 900 Hz, disturbances will be strongly attenuated and reference components will be followed at an improved accuracy. In this example we have just one notch shape. More may be required for multiple disturbance rejection and reference enhancement. Such a concept is not unknown in control engineering. However, *the levels of design intuition*, *achievable performances*, *stability requirements*, *and algorithm flexibility differ greatly in different controller constructions*.

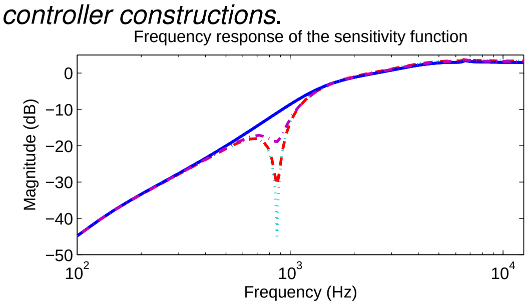

FIGURE 3. A sample customized loop shape

Among the set of all controllers that stabilize the plant, it is desired to choose the best possible design for implementation. Youla parameterization provides a convenient way to realize this concept.

Theorem 1 *Define the set **S**:={stable, proper, and rational transfer functions}. A single-input-single-output system $P(z^{-1})$ can be parameterized as $P(z^{-1}) = N(z^{-1})/D(z^{-1})$, where $N(z^{-1})$ and $D(z^{-1})$ are coprime over **S**, meaning there exists $U(z^{-1})$, $V(z^{-1})$ in **S** such that $U(z^{-1})N(z^{-1}) + V(z^{-1})D(z^{-1}) = 1$. If $P(z^{-1})$ can be stabilized by a negative feedback controller $C(z^{-1}) = X(z^{-1})/Y(z^{-1})$, with $X(z^{-1})$ and $Y(z^{-1})$ coprime over **S**, then* any stabilizing feedback controller *can be parameterized as*

$$\frac{X(z^{-1}) + D(z^{-1})Q(z^{-1})}{Y(z^{-1}) - N(z^{-1})Q(z^{-1})},\ Q(z^{-1}) \in \mathbf{S}. \quad (1)$$

This powerful concept suggests us the following design concept for precision motion control: (i) design first a baseline controller that satisfies the performance requirement under basic operations (e.g., one that achieves a common loop shape as shown in Fig. 2); (ii) apply Youla parameterization and introduce a customized $Q(z^{-1})$ to modify the servo loop under different servo requirements.

CUSTOMIZED YOULA PARAMETERIZATION FOR PRECISION MOTION CONTROL

By adopting the concept of Youla parameterization, we obtain very simple *stability requirements* (just need Q to be stable) and strong *algorithm flexibility* (all controllers can be parameterized by (1)). This section discusses further customizations to extend the *design intuition* and *achievable performance*. A realization of the control scheme using controller (1) is shown in Fig. 4. Three sets of elements need to be constructed to close the loop: the design of the baseline controller $C(z^{-1})$, the plant parameterization, and the choice of $Q(z^{-1})$ in (1). In the context of precision motion control, we propose the following design steps:

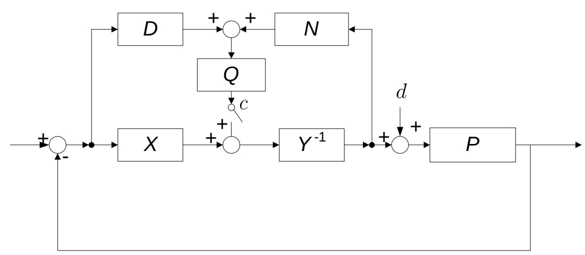

FIGURE 4. Block diagram of the feedback control system with Youla parameterization

step 1: use standard loop-shaping techniques such as PID, lead-lag, or H_∞ control to design a stable $C(z^{-1})$ for a baseline servo loop. The controller coprime factorization can then be simply chosen as $X(z^{-1}) = C(z^{-1})$ and $Y(z^{-1}) = 1$ in Fig. 4. Besides its simplicity, such a factorization brings increased design and tuning intuitions. Noting that $Y(z^{-1}) = 1$, if we lump all disturbances at the plant input, then the purpose of the customized Youla parameterization is to use the output of Q (the signal denoted by c in Fig. 4) to approximate $-d$ for disturbance cancellation. The output of Q can thus serve as an observed disturbance signal for algorithm verification and tuning. For instance, when testing the system offline via simulation, we can compare c and $-d$ to see if they match before closing the switch after the Q block. In the reference-tracking case, when there is imperfect tracking, the signal c can serve to explain the equivalent disturbance for identifying the critical errors.

step 2: factorize the discrete-time plant model by

$$P(z^{-1}) = z^{-m}P_n(z^{-1}) = z^{-m}/P_n^{-1}(z^{-1}) \quad (2)$$

so that $N(z^{-1}) = z^{-m}$ and $D(z^{-1}) = P_n^{-1}(z^{-1})$ in Fig. 4. Here $P_n^{-1}(z^{-1})$ should be stable for a valid coprime factorization. This is usually easy to satisfy for motion control systems. If the inverse plant is indeed unstable, we can use a stable version to approximate it. As a design example that will be used in the case-study section, if

$$P(z^{-1}) = z^{-2}\frac{3.4766 \times 10^{-7}(1 + 0.8z^{-1})}{(1 - z^{-1})^2} \quad (3)$$

then $P_n^{-1}(z^{-1}) = (1 - z^{-1})^2/3.4766 \times 10^{-7}/(1 + 0.8z^{-1})$, whose poles are already inside the unit circle. Hence we can choose the following coprime factorization $N(z^{-1}) = z^{-2}$, $D(z^{-1}) = (1 - z^{-1})^2/[3.4766 \times 10^{-7}(1 + 0.8z^{-1})]$.

step 3: with the discussed choices of $X(z^{-1})$, $Y(z^{-1})$, $N(z^{-1})$, and $D(z^{-1})$, the extended feedback controller in (1) becomes $\tilde{C}(z^{-1}) = [C(z^{-1}) + P_n^{-1}(z^{-1})Q(z^{-1})]/[1 - z^{-m}Q(z^{-1})]$. Using (2) and after some algebra, we can derive the new sensitivity function

$$\tilde{S}(z^{-1}) = \frac{1}{1 + P(z^{-1})\tilde{C}(z^{-1})} = \frac{1 - z^{-m}Q(z^{-1})}{1 + P(z^{-1})C(z^{-1})} \quad (4)$$

Although multiple elements have been added to the baseline loop, (4) is quite simple as it differs from the original sensitivity function $S(z^{-1}) = 1/(1+P(z^{-1})C(z^{-1}))$ only by a multiplicative term $1 - z^{-m}Q(z^{-1})$. To introduce small magnitude response in Fig. 2, we just need to design $Q(z^{-1})$ such that $1 - e^{-j\omega m}Q(e^{-j\omega})$ has low gains at the interested frequency region. This helps to provide intuitive designs that reach high achievable performances. Well-formulated tools such as internal model principle, Diophantine/Bezout equation, and convex optimization can be applied to design $Q(z^{-1})$ [3-6]. Relevant examples for precision motion control include:

(i) Active vibration rejection: although precision systems commonly include vibration-absorbing elements such as vibration isolation tables, passive damping and spring elements have a physical bandwidth above which they can not respond fast enough for energy absorption. There are also environmental disturbance that heavily depends on the operation condition and can even be time-varying. The loop shape in Fig. 3 suits for attenuating these vibrations actively from the control perspective. The different attenuation levels in the dash/dotted lines can be easily achieved by configurations in $Q(z^{-1})$. Additionally, we can observe that, when strongly attenuating disturbances at a local frequency region, the sensitivity function S did not have visible large amplification at other frequency regions. The essential design in this scheme is to assign $1 - z^{-m}Q(z^{-1})$ a notch-filter structure. Depending on the width of the desired notch, we can classify the problem to rejections of narrow-band disturbances [3,4] and general band-limited vibrations [6].

(ii) Repetitive control: this is common in manufacturing process where the majority of operations are repetitive. From Fourier series theory, any periodic disturbance or reference can be decomposed to summations of sinusoidal components at multiples of a fundamental frequency. For the feedback loop to have enhanced servo performance at these repetitive frequencies, we can let $1 - z^{-m}Q(z^{-1})$ have a comb shape in the magnitude response (see Fig. 6). This can be achieved by careful pole-zero placement in $1 - z^{-m}Q(z^{-1})$, via internal model principle [5].

(iii) Bandwidth extension: if the original baseline design $C(z^{-1})$ is too conservative, the proposed scheme can serve as a bandwidth-extension element. This can be readily done by assigning a low-pass filter structure to $Q(z^{-1})$, which will make $1 - z^{-m}Q(z^{-1})$ a high-pass filter.

CASE STUDY ON A WAFER SCANNER

Successful implementations of vibration rejection, repetitive disturbance cancellation, and periodic trajectory tracking have been obtained on a wafer-scanner testbed as shown in Fig. 5. This is an essential equipment in the semiconductor industry.[1] Due to limited space, we discuss below details about just the periodic tracking results on the reticle stage.

The plant has a continuous-time model $P(s) = 1/(0.2556s^2 + 0.279s)$. After discretization at a sampling time of $T_s = 0.4$ ms, the zero-order-hold equivalent of $P(s)$ has the structure of $k(z + 1)/[z(z - 1)^2]$, where k is a constant. Due to computation delays and signal processing, there is an additional one-step delay for $P(z^{-1})$. The zero at -1 makes the nominal inverse of $P(z^{-1})$

[1] There are two stages in the system: a wafer stage and a reticle stage, both capable of two-DOF plane motions. In the testbed one axis is set up in each stage for algorithm test.

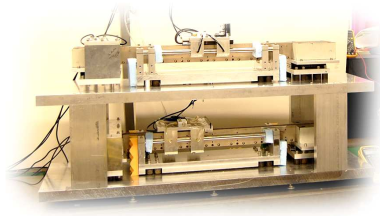

FIGURE 5. A testbed of wafer scanner system

marginally stable. Replacing it with a stable one at -0.8 and adjusting k so that the system gain matches that of $P(s)$ at low frequencies, we obtain the nominal plant model discussed in (3). This slight modification of the system zero at frequencies far above the system bandwidth does not yield much modeling errors in the frequency domain, and makes z^{-2} and $P_n^{-1}(z^{-1})$ a valid coprime factorization of (3).

The baseline controller is a PID controller $C = 10000[1 + 2T_s/(1 - z^{-1}) + 0.012(1 - z^{-1})/T_s]$. It stabilizes the loop and provides a baseline sensitivity function in the shape of Fig. 2. Letting the wafer scanner repeatedly track a scanning trajectory, we obtain the tracking error as shown in the dashed line in Fig. 7, where we can directly observe the periodic pattern for the error signal.

Recall the loop-shaping idea in Fig. 3 and the discussion in item (ii) in the last section. If we add the shape in the top plot of Fig. 6 to the baseline Fig. 2, we can reduce the periodic errors at multiples of the fundamental frequency. The Q filter to achieve Fig. 6 is [5]

$$Q\left(z^{-1}\right) = \frac{\left(1-\alpha^N\right) z^{-(N-m-n_q)}}{1-\alpha^N z^{-N}} z^{-n_q} q\left(z, z^{-1}\right)$$

which is a special periodic signal extractor as shown in the bottom plot of Fig. 6. Here m is the plant delay in Youla parameterization; N is the period of the trajectory; $q(z, z^{-1})$ is a zero-phase low-pass filter with order n_q; and α is a design parameter that controls the width of the comb shapes. An α closer to 1 gives a flatter shape for $1 - z^{-m}Q(z^{-1})$ (reduced amplification of the non-repetitive disturbances). A trade off in this case is that the algorithm requires more accurate knowledge about the period of the disturbance/trajectory. After the proposed compensation scheme is turned on, the errors in Fig. 7 are significantly reduced to be two-magnitude lower than the original values.

ACKNOWLEDGMENT

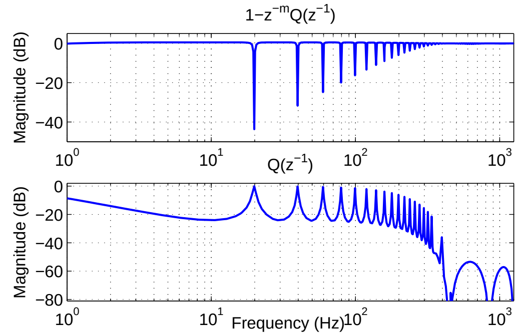

FIGURE 6. A Q-design example

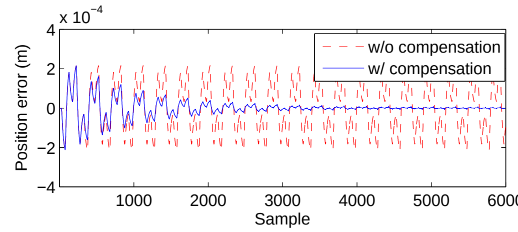

FIGURE 7. Tracking errors

The authors thank the support from CML at UC Berkeley, Nikon, Agilent Technologies, and National Instruments.

REFERENCES

[1] Advanced Manufacturing Portal, http://www.manufacturing.gov

[2] Tan K., et. al. Precision motion control: design and implementation. Springer, 2008.

[3] Chen X. and Tomizuka M., Adaptive Model Inversion For Rejection of Time-varying Vibrations On A Benchmark Problem, to appear in The European Control Conf. 2013, Jul. 17-19, 2013.

[4] ——, A Minimum Parameter Adaptive Approach for Rejecting Multiple Narrow-Band Disturbances with Application to Hard Disk Drives, IEEE Trans. Control Syst. Technol., vol. 20, no. 2, pp. 408-415, Mar. 2012.

[5] ——, New Repetitive Control with Improved Steady-state Performance and Accelerated Transient, to appear in IEEE Trans. Control Syst. Technol. 2013.

[6] Chen X., Oshima A., and Tomizuka M., Inverse Based Local Loop Shaping For Vibration Rejection In Precision Motion Control, to appear in The 6th IFAC Symposium on Mechatronic Syst., Apri. 10-12, 2013.